Zhu, Y.-F., Wei, H.-Z., Wang, J.-L., Williams-Jones, A. E., Wang, Z.-C., Jiang, S.-Y., Hohl, S. V., Huan, C., and Zhang, M.-M., 2023, Accurate Determination of Silver Isotopic Composition in Silicate Rocks with Low Silver Abundance: ACS Earth and Space Chemistry, v. 7, p. 2031-2041

Accurate determination of the silver isotopic composition of silicate rocks with low silver abundance

Yuan-Feng Zhu [a], Hai-Zhen Wei [a,b]*, Jun-Lin Wang [a], A. E. Williams-Jones [c], Zai-Cong Wang [d], Shao-Yong Jiang [d], Simon V. Hohl [e], Chun Huan [a], Miao-Miao Zhang [a]

[a] State Key Laboratory for Mineral Deposits Research, School of Earth Sciences and Engineering, Nanjing University, Nanjing 210023, PR China
[b] CAS Center for Excellence in Comparative Planetology, China, Anhui 230026, PR China[b]
[c] Department of Earth and Planetary Sciences, McGill University, Montreal H3A 0E8, Canada
[d] State Key Laboratory of Geological Processes and Mineral Resources, School of Earth Resources, China University of Geosciences, Wuhan 430074, PR China
[e] State Key Laboratory of Marine Geology, School of Ocean and Earth Science, Tongji University, Shanghai 200092, PR China

* Author to whom correspondence should be addressed:
Prof. Hai-Zhen Wei
School of Earth Sciences and Engineering, Nanjing University
163 Xianlin Avenue, Nanjing, Jiangsu, 210023 PR China
Phone: +86 (25) 89681617; Fax: +86 (25) 89682393

Email address: haizhenwei@nju.edu.cn

ABSTRACT

Owing to the extremely low abundance of silver in the Earth's crust and mantle, it is a major challenge to eliminate impurities from samples to obtain accurate silver isotopic data for silicate rocks. To achieve a precise and accurate determination of the silver isotopic composition of silicate rocks, we have modified the pre-treatment procedure and assessed isobaric interference and matrix effects, as well as analyzed silver isotopic compositions in silicates. By modifying the silicate digestion and ion-exchange procedures, an efficient elution of silver was achieved. The doping experimental results indicated that the matrix effect induced by Ti and Cr could be satisfactorily corrected using the internal standard Pd isotope pair of ^{108}Pd-^{106}Pd. The modified chemical chromatographic method effectively separates Ni from Ag in silicate samples, thereby minimizing significant isobaric interference from Ni cations. As a result, the shifts in δ^{109}Ag value caused by cations can be corrected to less than 0.02‰. There is a departure of up to 0.82‰ from the accepted δ^{109}Ag value when soluble metasilicate is present in the solution, which might explain the discrepancies in measured δ^{109}Ag for silicate materials. To accurately analyze silver isotopic compositions, especially of silicates with extremely low silver abundance, a silver standard doping method with an optimum doping proportion (sample to standard material of 2:8) has been shown to produce an acceptable measurement uncertainty from 0.04‰ to 0.06‰ (2SD). The high-precision δ^{109}Ag value determined in this study for ultramafic rocks from Balmuccia and the basalt reference material, BHVO-2, of -0.044±0.062‰ is consistent with that of -0.16±0.07‰ reported by previous studies. Our study paves the way for the more extensive use of silver isotopes in studies of terrestrial/extraterrestrial rocks, something that will be of help in constraining the sources of precious metals in polymetallic ore deposits as well as core formation and volatile-element depletion in the early solar system.

KEYWORDS: Silver isotopic analysis; ultramafic rocks; procedure recovery; matrix effect; isobaric interference

INTRODUCTION

As a ubiquitous trace element in most terrestrial and extraterrestrial rocks, silver shows both siderophile and chalcophile behavior in moderately volatile species.[1] It commonly exists in nature the form of native silver, or as alloys with gold, mercury, bismuth, copper, platinum, and as sulphides, sulfosalts and silver halides.[2-4] Silver has an atomic number of 47, an atomic weight of 107.8682, and consists of 28 radio isotopes with atomic weights ranging from 92.950 (^{93}Ag) to 129.950 (^{130}Ag) and two stable isotopes, ^{107}Ag (51.839(51)%) and ^{109}Ag (48.160(51)%).[5] The isotopic composition of stable silver is usually expressed as δ^{109}Ag (as per mil deviation) (Eq. 1) or ε^{109}Ag (as per ten thousandths deviation) (Eq. 2) relative to the NIST SRM 978a (AgNO$_3$), the widely accepted standard material for silver isotopes with the ^{109}Ag/^{107}Ag ratio of 0.92904 ± 0.00022 [6]:

$$\delta^{109}\text{Ag}=\left(\frac{({}^{109}Ag/{}^{107}Ag)_{sample}}{({}^{109}Ag/{}^{107}Ag)_{standard}}-1\right)\times 1000\text{（‰）}\quad\text{（Eq. 1）}$$

$$\varepsilon^{109}\text{Ag}=\left(\frac{({}^{109}Ag/{}^{107}Ag)_{sample}}{({}^{109}Ag/{}^{107}Ag)_{standard}}-1\right)\times 10000\text{（ε）（Eq. 2）}$$

Silver isotope geochemistry has advanced rapidly in the planetary sciences and geosciences in recent decades. During early research, silver isotopic compositions were particularly useful in studying volatile depletion in the early solar system because the extinct radionuclide ^{107}Pd decays to ^{107}Ag (half-life of 6.5 Ma).[7] The Pd−Ag chronometer has been successfully applied to study core formation and volatile-element depletion processes in the early solar system.[1,8-15] More recently, with an improved understanding of the fractionation mechanisms of silver isotopes in processes affecting the environment, δ^{109}Ag values have been applied as a sensitive tool with which to track the sources and paths of migration of silver contaminants.[16-21] The narrow range of δ^{109}Ag silver isotope ratios in silver coins from different periods, [22-28] and minimal metallurgical isotopic fractionation, [29] make silver isotopes excellent recorders of the provenance and circulation of past silver coinages.[22, 24-27] In contrast, the range of δ^{109}Ag values of silver ores deposits is much greater (δ^{109}Ag = -1.0 to +2.3‰).[29-32] Studies related to the genesis of polymetallic mineral deposits have indicated that there is no systematic δ^{109}Ag variation with the age of mineralization, deposition temperature, deposit-type or the nature of the source rocks.[33] Instead, physicochemical processes related to silver transport and deposition control silver isotopic fractionation during ore formation,[27, 29, 33-35] which allows for δ^{109}Ag to be applied to the study of the genesis of base and precious metal deposits and in their exploration.[29-31, 35]

Silver has been mined and extracted since ancient times and, like gold, has been widely considered to be a precious metal. As early as 79 A.D., Pliny the Elder noted that “in every species of gold there is a proportion of silver, in some one-tenth part, in others a ninth”.[36] In recent years, the demand for gold and silver has increased sharply. Gold and silver occur mainly as native gold or native silver in ore deposits, but silver may also occur as the sulfides, acanthite and argentite, and with gold in more complex minerals containing other elements .[32-33, 37-38] Several studies have shown that both gold and silver are highly soluble as bisulfide and chloride complexes in hydrothermal systems.[29, 34, 39-46] The similarity of the chemical properties of gold and silver makes δ^{109}Ag an ideal tool for quantitatively evaluating the formation of mineral deposits involving gold.[47]

The stable silver isotope ratio was firstly determined by Chen and Wasserburg,[48] using thermal ionization isotope mass spectrometry (TIMS), to a precision of 1 to 2‰, providing significant evidence for the existence of the extinct isotope, ^{107}Pd, in the early solar system because of the excellent correlation between ^{107}Ag/^{109}Ag and Pd/Ag.[48-52] However, the analysis of Ag by TIMS does not provide a means for correcting the instrument-induced mass fractionation because Ag has only two stable isotopes.[53] This precludes using this method of analysis in Pd-Ag chronometers at moderate to low Pd/Ag ratios (<10000) and in terrestrial processes that produce a variation of only a few per mil in δ^{109}Ag.[37, 54] To improve precision in the determination of Ag isotopic composition, Carlson and Hauri[53] used multiple-collector inductively coupled plasma mass spectrometry (MC-ICP-MS) to determine the silver isotopic compositions of meteorites with a low Pd/Ag ratio, and obtained an improvement in analytical precision of ±0.13‰ or better on Ag samples of 25 to 50 ng or greater. To achieve an accurate determination of the silver isotopic composition of basalts and meteorites, Schönbachler et al.[54] designed a three-stage ion-exchange procedure to completely separate Ag from Ti and Fe and other matrix elements. They achieved an external reproducibility of ±0.05‰, and thoroughly evaluated the instrumental mass discrimination in the presence of matrix elements with dry plasma versus wet plasma. Yang et al.[18, 55] and Luo et al.[17] achieved an efficient purification of Ag using a two-column ion-exchange procedure, obtaining an external reproducibility of ±0.04‰ for commercial Ag products and better than ±0.015‰ for environmental material. A recent modification in our laboratory of the chemical chromatographic and two-step ion exchange process for separating and purifying ore deposit samples has enabled us to separate and purify silver from base-metal matrices, thereby ensuring accurate silver isotopic analysis of ore samples with an external reproducibility of 0.009 to 0.084‰.[37]

Although there have been numerous studies of the distribution of δ^{109}Ag values in polymetallic ore deposits,[11, 27, 31, 33, 35, 37, 47, 56-57] the Ag isotopic compositions of the major reservoirs of the Earth (such as the crust and mantle) are still not well-constrained. The large differences in the silver isotope ratio reported for the Hawaiian basalt sample (KOO49), e.g., δ^{109}Ag values of +1.057±0.025‰[54] and -0.574±0.012‰[11] provides evidence for isotopic fractionation during the digestion or purification procedures used in extracting Ag from silicate rocks. Such inconsistencies in isotopic composition also were observed in repeated analyses of granites in our study. [29] Because silver is a trace element in silicate rocks, the large differences in silver abundances measured for suites of the same rock-type may not be statistically significant. For example, the silver concentration is ca. 8 $ng\cdot g^{-1}$ in the primitive mantle,[58] 19 $ng\cdot g^{-1}$ in the mantle,[1] 9±3 $ng\cdot g^{-1}$ in the bulk silicate Earth (BSE) [58] and ca. 56 $ng\cdot g^{-1}$ in the upper crust.[59] Thus, the extremely low abundance of silver in silicate rocks and high contents of metals such as Ti, Cr and Ni, which are at two to six orders of magnitude more abundant than silver (Table S1), could make it difficult to accurately determine the silver isotopic composition of silicate rocks.

Until now, few studies have been dedicated to silver isotopic analysis in silicate rocks in geological settings.[1, 11, 54] Owing to the small number of datasets, establishing the silver isotope characteristics of the Earth's major reservoirs continues to be challenging. In this study, we present a new high-precision approach to stable silver isotope analysis for silicate samples with low silver abundance. This includes the modification of the sample pre-treatment and ion exchange chromatography, the quantitative evaluation of matrix effects and isobaric interferences from impurities, and the development of a standard material doping approach with an optimum doping proportion. Using this modification, we have obtained high-precision silver isotopic analyses for ultramafic rocks and standard reference materials that serve to validate its use in future silver isotopic analyses of silicate rocks with low silver contents.

EXPERIMENTAL SECTION

Preparation of samples

Milli-Q water (resistivity = 18.2 MΩ·cm) was used throughout the experiments, and concentrated HCl and HNO_3 were prepared through repeated sub-boiling distillation of commercial acids (AR) using Savillex distillers. A NIST SRM 978a standard solution from the National Institute of Standards and Technology (NIST), was selected as the "zero" reference standard for silver isotopic analysis in this study. The reported absolute silver isotope ratio is $^{109}Ag/^{107}Ag = 0.92904 \pm 0.00022$, and the nuclide mass of ^{107}Ag and ^{109}Ag is 106.905095 and 108.904754, respectively.[6] For our experiments, a NIST SRM 978a solution of 1000 $\mu g \cdot mL^{-1}$ (ppm) was prepared in a 2% (v/v) HNO_3 solution, diluted to 100 $ng \cdot mL^{-1}$ (i.e., 100 ppb) and stored in a light-protected Teflon bottle. Additionally, a pure silver solution (AG-NJU) from the China National Non-ferrous Metals and Electronic Materials Analysis and Testing Centre was checked for the homogeneity of its silver isotopic composition via repeated duplicate analyses (n > 30) and was used as an in-house silver isotope reference material in our laboratory.

A synthetic silver solution that acted as an analogue to silicate rocks was prepared for this study, using the average metal abundances of the upper crust.[60] A solution of the internal standard, AG-NJU, was prepared in a solution medium of 2% (v/v) HNO_3, and was then mixed with other pure metal solutions (such as Cr, Cu, Ni, Pb, Zn, Fe and Ti) to prepare a 40 mL of synthetic solution with an Ag concentration of 250 ppb. The molar ratios of metal to Ag and the contents of each element in the solution are reported in Tables S1, S2. The standard, NIST SRM 3138 ($PdCl_2$, LotNo.090629), from the National Institute of Standards and Technology (NIST) was used as an internal standard to correct for instrument-induced mass bias during the determination of silver isotopic compositions.

Four silicate rocks from the Balmuccia peridotite massif in the Italian Alps were employed in this study. The Balmuccia pyroxenites, which are from a fragment of the subcontinental lithospheric mantle are interpreted to be the products of melt–peridotite reaction and the subsequent accumulation of pyroxene, spinel and garnet plus accessory phases in the subcontinental lithospheric mantle.[61] This mantle tectonite was emplaced into lower crustal granulite facies metabasites of the Ivrea–Verbano zone (IVZ) and subsequently exposed at the surface during the course of Mesozoic extension and Alpine compression. A detailed description of the samples, and the concentrations of major and trace elements have been provided in previous studies of these samples.[58, 61-65] Additionally, a geological reference material basalt sample (BHVO-2) of the United States Geological Survey was prepared for silver isotopic analysis.

Whole rock digestion procedure

A multi-acid digestion procedure was used to fully dissolve the rock samples. Approximately 0.6 g of silicate rock sample powder was weighed and digested in a mixture of 3 mL of HF and 1.5 mL of HNO_3 in a closed Savillex Teflon beaker in an oven for two days at 190 °C. The samples, to which 3 mL of 6 M HNO_3 had been added, were then evaporated to dryness at 40 °C on a hot plate. This was followed by the addition 3 mL of 6 M HCl to the beaker, which was heated on a hot plate of 110 °C to complete the dissolution. The solution was then centrifuged at 1500 rpm for ten minutes and the supernatant liquid was diluted in 30 mL of 0.5 M HCl. This whole rock digestion procedure ensured that the geological standards and silicate rock samples had dissolved completely.

Ion-Exchange Chromatography

To separate and purify trace silver from the silicate rocks, we made use of a previously described one-step ion-exchange procedure that was modified as described below.[11, 17, 37, 54]. A 1 mL aliquot of anion exchange resin (AG1-X8, Biotechnology grade, Bio-Rad Laboratory, 100-200 mesh) was loaded into a 10mL polypropylene Muromac® column with an internal diameter of 5 mm, which had been cleaned and pre-conditioned with 30 mL of 2 M HCl and then15 mL 0.5 M HCl. An aliquot of the sample solution was then loaded onto the pretreated columns. The matrix elements were eluted successively with 50 mL of 0.5 M HCl, 30 mL of 0.1 M HCl and 15 mL of 0.01 M HCl. The columns were then rinsed with 5 mL of 0.2 M HNO_3 to remove the residual cation matrices including Pb, Zn, Cu, Cr, and Fe, and the Ag was eluted from the resins with 5 mL of 0.2 M HNO_3 and 10 mL of 6.0 M HNO_3. Details of the ion-exchange procedure are given in Table 1.

Table 1. Silver separation and purification procedure for the silicate rocks

Step	Procedure	Reagents	Dosage (mL)
1	Column loading	AG1-X8	1
2	Cleaning	2M HCl	30
3	Pre-conditioning	0.5 M HCl	15
4	Sample loading	Sample solution	1
5	Rinsing matrix	0.5 M HCl	50
6	Rinsing matrix	0.1 M HCl	30
7	Rinsing matrix	0.01 M HCl	15
8	Eluting cations	0.2 M HNO3	5
9	Eluting Ag	0.2 M HNO3	5
10	Eluting Ag	6.0 M HNO3	10

Elemental composition analysis

The elemental contents of the elutants were analyzed using an ICP-MS (Finnigan Element II) and ICP-OES (Agilent-7100) at the Nanjing Institute of Geology and Palaeontology, Chinese Academy of

Sciences (NIGPAS). The signal drift during ICP-MS measurements was corrected by adding Rh internal standard solutions of known concentration with an analytical reproducibility better than ± 5%. As the concentration of Fe in the solution was at the ppm level, ICP-OES was used to analyze for the Fe concentration, for which the error was ±3%.

Doping experiment

Using the ion-exchange procedure developed in our previous study, we were able to effectively remove the matrix ions that induce possible isobaric interferences with silver isotopes (e.g., $^{65}Cu^{40}Ar^{+}$, $^{66}Zn^{40}Ar^{+}$, $^{67}Zn^{40}Ar^{+}$, $^{68}Zn^{40}Ar^{+}$, and Pb^{2+}); the molar ratios, Fe/Ag, Zn/Ag, Cu/Ag, and Pb/Ag were less than 0.723, 0.066, 0.016, and 0.183 mol/mol, and thus were below the level of metal impurities that could be tolerated (i.e., Cu/Ag ≤ 50:1, Fe/Ag ≤ 600:1, Pb/Ag ≤ 10:1, and Zn/Ag ≤1:1, respectively).[37] However, this did not exclude the possibility that isobaric interferences and matrix effects due to the presence of other metal impurities (e.g., Ti, Cr and Ni) characterized by high metal/Ag molar ratios might influence the silver isotopic analysis (Table S1). To better assess this complex matrix effect when determining the silver isotopic composition of silicate samples, pure solutions of Cr^{3+}, $Ni^{2+}$and Ti^{4+} from the National Non-ferrous Metals and Electronic Materials Analysis and Testing Center of China were added to a NIST SRM 978a solution. With reference to the silver elution curves in our preliminary experiment, we prepared a series of solutions containing 100 ppb of Ag with molar ratios of Ti/Ag from 0:1 to 600:1, Cr/Ag from 0:1 to 2000:1, and Ni/Ag from 0:1 to 200:1. In Addition, a batch of experiments were prepared by adding Si to the NIST 978a solutions having Si/Ag molar ratios from 0:1 to 1000:1 to evaluate the matrix effect of Si.

Silver isotopic analysis

We used a Neptune Plus MC-ICP-MS (Thermo Fisher Finnigan) with an ESI PFA 50 µL/min nebulizer in a quartz cyclonic spray chamber to measure the silver isotopic composition. The signals of $^{107}Ag^+$ and $^{109}Ag^+$ ions were detected by Faraday cups C and H2, and $^{104}Pd^+$, $^{105}Pd^+$, $^{106}Pd^+$, and $^{108}Pd^+$ ions were detected by Faraday cups L3, L2, L1 and H1, using 10^{11} Ω amplifiers. The mass bias was corrected via sample-standard-bracketing with an internal normalization procedure (C-SSBIN) described by Luo et al.[17]. A 2 µg·mL^{-1} internal Pd standard was added to the standard solution containing 100 ng·mL^{-1}Ag in the Ag/Pd molar ratio of 1:20, which was determined to be optimal for mass bias correction.[37] The silver content in both the sample solution and the NIST SRM 978A standard solution was ~ 100 ppb, resulting in a signal of ∼2.2 V on $^{107}Ag^+$ with the conventional H-skimmer cone. The $^{104}Pd^+$ signal was ~ 8V and the $^{105}Pd^+$ signal was ~ 16V. To avoid memory effects, we washed the inlet system with 3% HNO_3 and then Milli-Q water for ∼10 min between measurements. This reduced the background signal to ∼3 mV.

To determine the silver isotopic composition by MC-ICP-MS, we used a palladium solution as an internal standard for mass bias correction; the samples were doped with this solution before analysis. Natural palladium (Pd) has six stable isotopes, namely ^{102}Pd, ^{104}Pd, ^{105}Pd, ^{106}Pd, ^{108}Pd and ^{110}Pd. Except for two theoretically unstable isotopes (^{102}Pd and ^{110}Pd), the other isotopes have the following relative isotopic abundances, ^{104}Pd (0.1114 (8)), ^{105}Pd (0.2233 (8)), ^{106}Pd (0.2733 (3)), and ^{108}Pd (0.2646 (9)). Theoretically, the similar isotope abundances of the stable Pd isotopes make any isotope pair (e.g., ^{104}Pd–^{105}Pd, ^{104}Pd–^{106}Pd, ^{104}Pd–^{108}Pd, ^{105}Pd–^{106}Pd, ^{105}Pd–^{108}Pd, and ^{106}Pd–^{108}Pd) suitable for mass bias correction in the absence of isobaric interferences. The correction formula is provided in Eq. 3 and Eq. 4:

$$\beta = \frac{\ln\left(({}^{j}Pd/{}^{i}Pd)_{True}/({}^{j}Pd/{}^{i}Pd)_{Measure}\right)}{\ln\left(\frac{m_j}{m_i}\right)} \quad \text{（Eq. 3）}$$

$$\frac{{}^{109}Ag}{{}^{107}Ag}_{True} = \frac{{}^{109}Ag}{{}^{107}Ag}_{Measured} \times \left(\frac{m_{109}}{m_{107}}\right)^{\beta} \quad \text{（Eq. 4）}$$

where the subscripts represent the measured and corrected isotope ratios, and β is the correction factor for mass bias. The absolute masses of m_{107} and m_{109} are 106.905095(^{107}Ag) and 108.904754(^{109}Ag),[66] respectively. The parameters ^{i}Pd and ^{j}Pd are the internal standard pairs, ^{104}Pd-^{105}Pd, ^{104}Pd-^{106} Pd, ^{104}Pd-^{108} Pd, ^{105}Pd-^{106} Pd, ^{105}Pd-^{108} Pd and ^{106}Pd-^{108}Pd, respectively, and m_j and m_i represent the absolute atomic mass of Pd as103.90404(^{104}Pd), 104.90509(^{105}Pd), 105.90349(^{106}Pd), 107.90389(^{108}Pd).[67]

A 800 μg·mL^{-1} Pd working standard solution of the standard material, NIST SRM 3138 ($PdCl_2$), referred to above was freshly prepared for each analytical session by quantitative dilution of a stock solution in 2% (v/v) HNO_3. The Pd solution was added to both the sample and Ag standard solutions as a common doping matrix and as an internal standard for mass bias correction. Mass discrimination and instrument drift were corrected by a combination of internal normalization with Pd and standard-sample bracketing.

The reproducibility referred to in this study is based on repeated measurements of the samples (n ≥ 5, 2SD, 95% confidence limit). The average internal analytical precision (n = 40, 4 blocks × 10cycles) of the measured ^{109}Ag/^{107}Ag ratios of 100 ng·mL^{-1} NIST SRM 978a is ±0.02‰ and the long-term external reproducibility is 0.012‰ (n ≥ 10, 2SD). The external reproducibility achieved in this study of the geological standard material, NIST SRM 978a, the laboratory internal standard material, AG-NJU, the synthetic solution and the silicate rocks are 0.03 to 0.05‰ (n ≥ 10, 2SD), 0.05 to 0.06‰ (n ≥ 10, 2SD) (Figure 1a), 0.08 to 0.11‰ (n ≥ 10, 2SD) (Figure 4), and 0.03 to 0.07 ‰ (n ≥ 10, 2SD) (Figure 8), respectively.

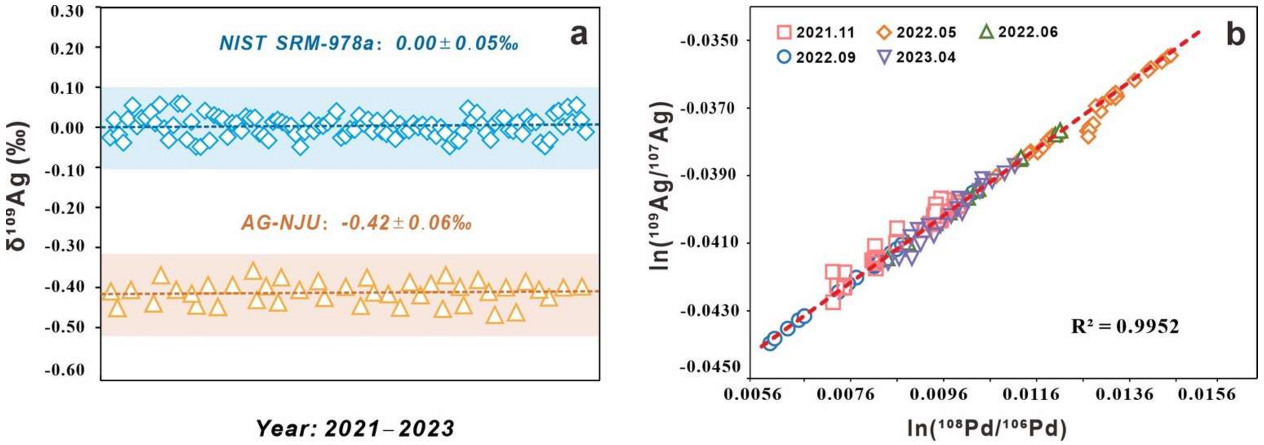

Figure 1. (a) The reproducibility of the silver isotopic analyses of the standard reference materials, NIST SRM 978a and AG-NJU; and (b) the correlation of ln (^{109}Ag/^{107}Ag) with ln (^{108}Pd/^{106}Pd) for silver isotopic analyses over the long-term.

RESULTS AND DISCUSSION

The influence of silver loss on the determined ^{109}Ag/^{107}Ag ratios

This study revealed an apparent silver loss accompanied by abnormally high ^{109}Ag/^{107}Ag ratios if samples with a low silver concentration were separated and purified using the procedures employed in analyzing silver-bearing minerals and meteorites. As shown in Figure 2a, the ^{109}Ag/^{107}Ag ratios are as high as 1.2033 if the silver recovered from the column is less than 6% of the sample mass, which is well beyond the range of silver isotopic ratios (X -Y) observed in terrestrial samples. From a compilation of the experimental data, it is evident that the measured silver isotopic ratio follows a closed-system Rayleigh distillation model (Eq. 5), which yields a silver isotopic fractionation factor $\alpha_{\text{resin-elution}}$ of 0.9496 (Figure 2a). This implies that the light ^{107}Ag isotope prefers the resin to the eluent during ion-exchange, and that incomplete elution of the silver from the resin induces significant silver isotopic fractionation.

$$\delta^{109}Ag_{elution} + 1000 = (\delta^{109}Ag_0 + 1000)\frac{1-f^{\alpha}}{1-f} \quad \text{(Eq. 5)}$$

where $\delta^{109}Ag_{elution}$ and $\delta^{109}Ag_0$ are the silver isotope values after elution and of the initial solution, respectively, *f* is the fraction of silver remaining in the resin; α is the silver isotopic fractionation factor between the eluent and the resin.

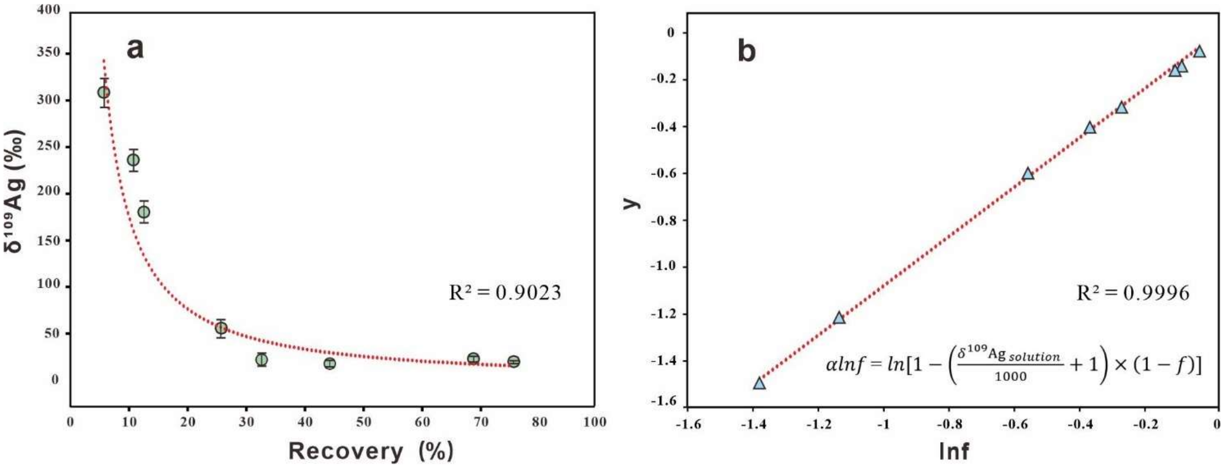

Figure 2. (a) The change in $\delta^{109}Ag$ in the eluent with the percentage of silver recovery during elution; (b) the silver isotopic fractionation factor between the resin and the eluent and the corresponding Rayleigh distillation model for a closed system.

A modified ion-exchange procedure for the purification of silver from silicate rocks

It has been shown that the chemical chromatographic procedure employed in previous studies, which makes use of the AG1-X8 resin, can remove cations such as Fe, Cu, Cd, Sn, and Au effectively.[11, 17, 33, 37, 54] However, it also has been suggested that the large amounts of Ti compared to Ag might compromise the silver isotopic analysis.[54] Because of the extremely low abundance of silver in silicate rocks and the large impact that the chemical composition of the material can have on silver isotope ratios, we modified the ion exchange protocol of Theis and Schönbächler [11]. A set of experiments in which single aliquots of synthetic solution containing ca. 100-200 ng of Ag were loaded into the pretreated columns was performed to evaluate silver recovery and the efficiency of silver separation from the matrices. As shown by the elution curves (Fig. 3), use of the modified protocol presented in Table 1 ensured the efficient removal of most of the cations before silver elution, especially Ti, Fe, Ni, which that are present in significant concentrations in the ultramafic silicate rocks considered in this study (Table S1). The maximum recovery of silver from the column varied between 90.1% and 98.9%, based on estimates from multiple measurements (n > 5). This recovery was considered to be acceptable because of the uncertainty of ± 5% in measurements of the silver content using ICP-MS and the reduction in silver ion concentration in aqueous media induced by exposure to sunlight. However, the high Cr/Ag molar ratio (~196:1) shows that much of the Cr was not removed during elution. To avoid any shifts in the measured silver isotope ratios due the presence of Cr ions, the related matrix effect was assessed as discussed below.

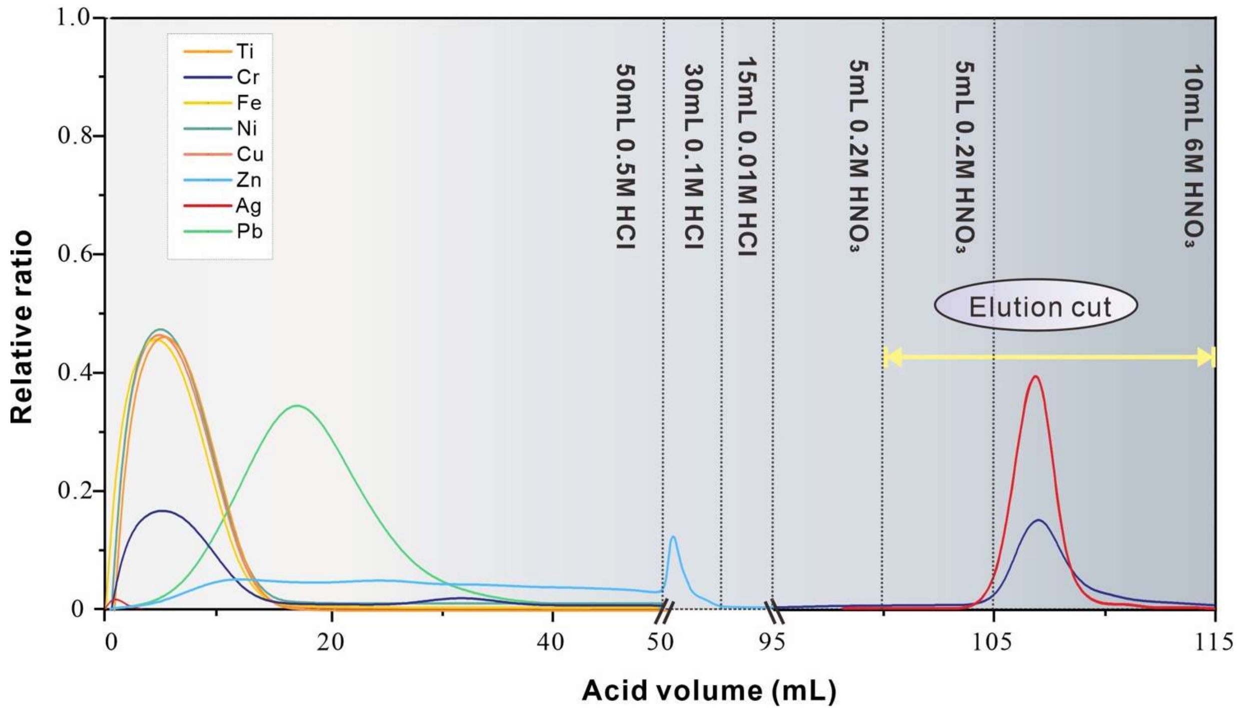

Figure 3. Elution curves for silver and other cations in the matrix of the synthetic solution after use of the modified ion exchange procedure.

The δ^{109}Ag value of a synthetic solution composed of the standard material, AG-NJU, which has a δ^{109}Ag value of -0.42±0.06‰, was measured before and after elution using the unmodified protocol (Figure 4). From the measured deviation of 0.54‰ ($\Delta^{109}Ag = \delta^{109}Ag_{measured} - \delta^{109}Ag_{ture}$), it is apparent that impurities in the solution affected the analyzed value of δ^{109}Ag significantly. After adoption of the modified protocol, the δ^{109}Ag value of the synthetic solution was determined to be -0.46±0.11‰ (i.e., the deviation decreased to 0.08), which is in excellent agreement with the accepted value of -0.42±0.06‰, showing that the silver isotopic composition of silicate rocks can be analyzed accurately using our modified protocol .

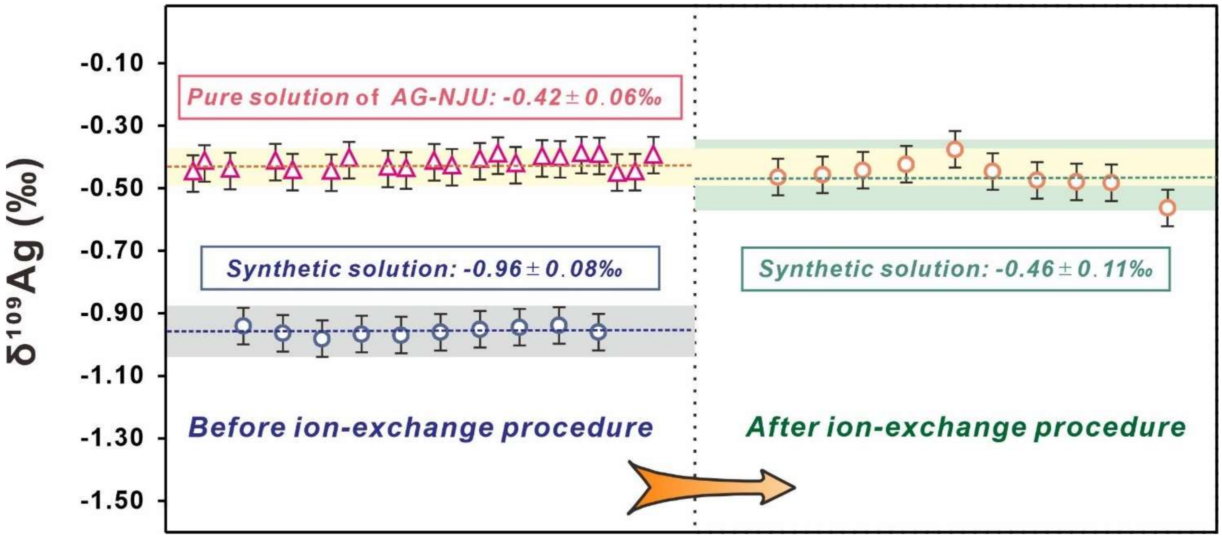

Figure 4. The measured silver isotope (δ^{109}Ag) ratio of a synthetic solution that contained AG-NJU before and after the modified ion-exchange procedure.

Matrix effects on silver isotopic analysis of silver in silicate rocks

The matrix effect produced by determining silver isotope ratios using MC-ICP-MS comes mainly from spectral (e.g., homotopic ion interference) and non-spectral interference, the latter of which is caused by a variety of factors, including differences in the composition of the natural sample and the synthetic (single-element composition) standard, i.e., concentration and redox state mismatches between the analyte and the standard as well as the presence of organic matter.[68] These interferences need to be considered for stable isotope systems because they may lead to mass deviations that affect the results. Previous studies have shown that the matrix effects of Na, K, W and Sn ions can be rendered negligible after mass bias corrections via the C-SSBIN procedure.[55] The matrix effects of Ir, Sm and Rb have been shown to increase the Pd-corrected Ag isotopic composition by approximately 0.1‰.[53] The isobaric interferences of Fe, Cu, Pb and Zn ions on Ag isotope measurements in silver-bearing minerals were assessed in our previous study.[37] To better evaluate the possible matrix effects from impurities of Ti, Cr, and Ni, we analyzed the NIST SRM 978a Ag standard solution doped with different ratios of these cations over Ag as samples.

As shown in Figures. S1, S2, S3, the correlations of ln (^{109}Ag/^{107}Ag) with ln (^{i}Pd/^{j}Pd) produce significant but different distributions of the analyzed ratios for the different Pd isotope pairs with increasing concentrations of cation impurities. Because of the isobaric interference of ^{64}Ni^{40}Ar^{+} with ^{104}Pd from the presence of Ni ions, the occurrence of matrix Ni^{2+} causes a noticeable shift in the measured δ^{109}Ag values. Moreover, there is a linear relationship of δ^{109}Ag with [Ni]/[Ag] with a slope of 0.0003 (R^2 = 0.987) (Figure 5a-b). However, an isobaric interference from Ni cations during the analysis of silver isotope ratios is eliminated using the modified ion-exchange protocol for silicate samples developed in this study because of the removal of most of the Ni (Figure 3). Thus, the Ni/Ag molar ratio was only 1.34:1 in the final eluent. By contrast, although the Ti/Ag and Cr/Ag molar ratios of the final eluent were as high as 600:1 and 2000:1, addition of the isotope pair of ^{108}Pd/^{106}Pd corrected the matrix effects from Cr and Ti such that the reproducibility of the silver isotope was within ±0.02‰. In conclusion, the matrix effect caused by Ti and Cr cations was satisfactorily corrected using the C-

SSBIN approach. (Figure 5c-f).

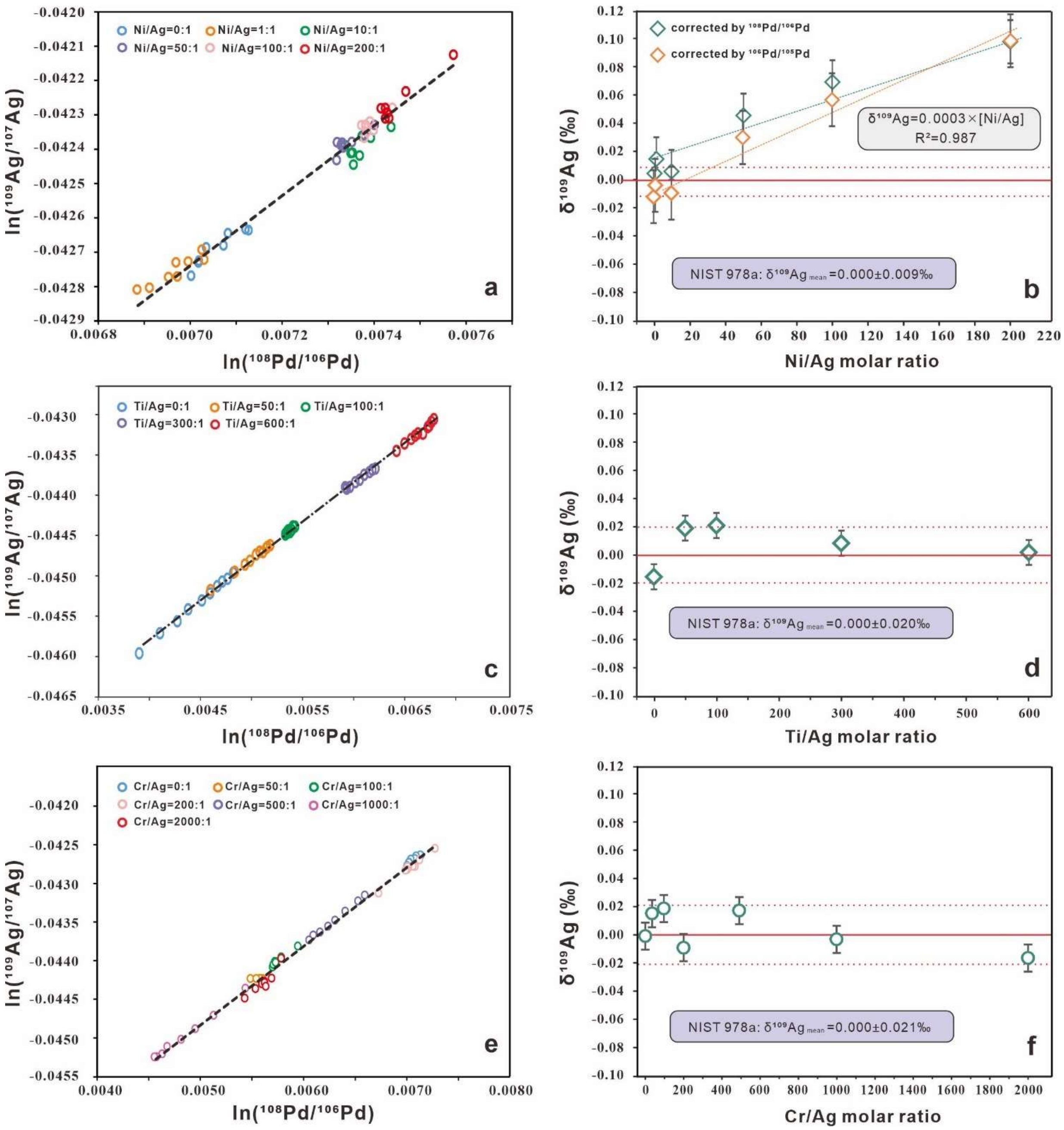

Figure 5. The correlation of ln ($^{109}Ag/^{107}Ag$) with ln ($^{108}Pd/^{106}Pd$) in the presence of nickel ions (a), titanium ions (c), and chromium ions (e); The matrix effects of Ni cations (b), Ti cations (d) and Cr cations (f) on the measured $\delta^{109}Ag$ values.

Bulk silicate Earth (BSE) has an average Si concentration of 16.1 wt.%,[69] and the upper crust an average Si concentration of 28.8 wt.%.[70] Consequently, the digestion of silicate rocks introduces a large amount of silicon into the solution. Moreover, metasilicate matrices have been shown to produce interferences in stable isotopic analysis, especially for $\delta^{11}B$.[71-74] However, the impact of silicate matrices on the accuracy of silver isotopic analyses has not been addressed. We, therefore, conducted a set of experiments to evaluate the Si matrix effect, in which Si was introduced into NIST 978a solutions to produce Si/Ag molar ratios from 0:1 to 1000:1.

The correlations between ln ($^{109}Ag/^{107}Ag$) and ln ($^{i}Pd/^{j}Pd$) with variable Si/Ag ratios are illustrated in Figure S3 and show that the isotope pair, $^{108}Pd/^{106}Pd$, performs better than other isotope pairs in correcting the metasilicate matrix effect and, for Si/Ag molar ratios below 600:1, can be used to ensure reliable $\delta^{109}Ag$ values with an external reproducibility of ±0.04‰ (Figure 6). For Si/Ag molar ratios greater than 1000:1, the beam signal becomes unstable. In our experiment, for which the Si/Ag molar ratio was 1000, the corresponding $\delta^{109}Ag$ value was 0.81 ‰ less than that of the standard and there was a pronounced decoupling of $^{109}Ag/^{107}Ag$ from $^{108}Pd/^{106}Pd$ (Figure 6). In summary, the matrix effect of soluble metasilicate can be effectively corrected using $^{108}Pd/^{106}Pd$ provided that the Si/Ag molar ratio is < 600:1.

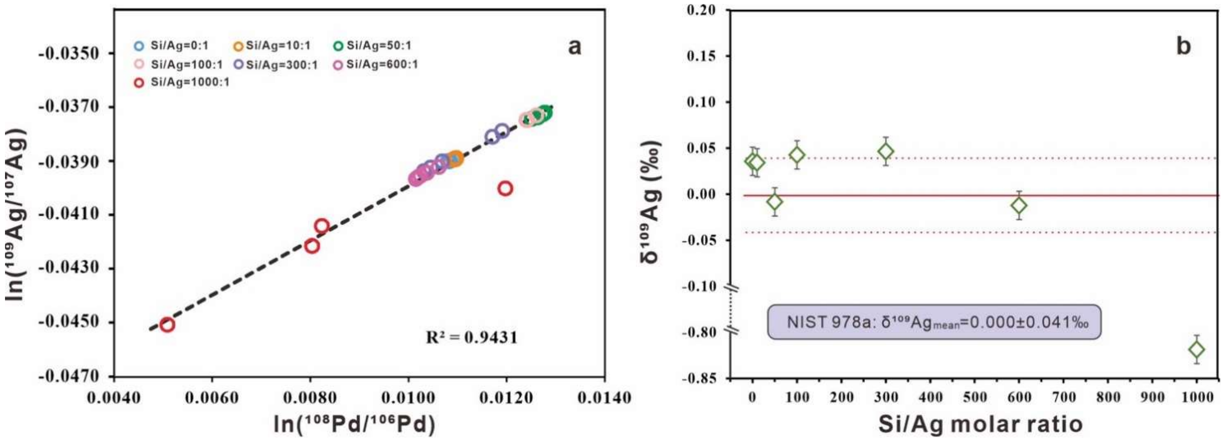

Figure 6. (a) The correlation of ln (^{109}Ag/^{107}Ag) with ln (^{108}Pd/^{106}Pd) in the presence of soluble metasilicate with variable Si/Ag ratios; (b) The matrix effect of soluble metasilicate on the measured δ^{109}Ag values.

An approach to silver isotope analyses of silicates with a low silver abundance

We propose the following protocol for analysis of the silver isotope composition of silicate samples with a silver content of a few ppb. This protocol involved doping the sample solution with standard reference material, AG-NJU having a δ^{109}Ag value of -0.42±0.06‰ and then conducting an ion exchange to make the silver content of the sample equivalent to that of the standard reference material, NIST SRM 978a. The correction procedure is based on the following mass balance equations:

$$R_i^{mix} = fR_i^{sample} + (1-f)\, R_i^{AG-NJ} \quad \text{(Eq. 6)}$$

$$\delta^{109}Ag_i^{mix} = f\delta^{109}Ag_i^{sample} + (1-f)\, Ag_i^{AG-NJU} \quad \text{(Eq. 7)}$$

where *f* is the proportion of silver in the sample and R_i^{sample} and R_i^{AG-NJU} are the mean ratios of ^{109}Ag/^{107}Ag in the sample and the silver standard solution, respectively; R_i^{mix} refers to the ratio of ^{109}Ag/^{107}Ag of a solution representing a mixture of the sample and standard solutions. The Ag isotopic composition of the samples is expressed as δ^{109}Ag, in per mil.

The correct silver isotopic value of the original sample is derived as follows:

$$\delta^{109}\mathrm{Ag}_{true} = \frac{\delta^{109}\mathrm{A}_{measured}}{f} - \frac{1-f}{f} \times \delta^{109}\mathrm{Ag}_{AG-NJU} \quad \text{(Eq. 8)}$$

Equation 6 is based on the mixing law equation of the double spike method, which is applied to multi-isotope systems.[76] The error evaluation and its propagation are conducted routinely in geochronology and isotope geology.[75, 77-78] In a departure from the method of error evaluation and propagation for the double spike technique,[76] Considering our external reproducibility of ±0.04‰ (2σ) from duplicate analyses and the internal precision of ±0.011‰ (SE) from single silver isotopic measurements of natural samples (Figure 7), the optimum doping ratio of sample to standard material is 2:8. Using this ratio, the measurement uncertainty is 0.04 to 0.06‰ (2SD). In this study, the standard doping approach was validated by doping the reference material, NIST SRM 978a, with the in-house silver isotope reference material (AG-NJU). Multiple measurements yield a mean δ^{109}Ag value of -0.002±0.058‰ (n>5) for NIST SRM 978a after elution, thereby confirming the reliability of the doping approach proposed here. The bulk silicate Earth (BSE) has been estimated to have a very low Ag concentration (4-8 ppb) [82] , which makes it very challenging to ensure that all the silver is recovered during digestion. Moreover, the modified ion-exchange procedure discussed here requires the loading of at least 100 ng of Ag into the pretreated columns, which is equivalent to a minimum silver abundance in the rock of 40 ng·g^{-1}.

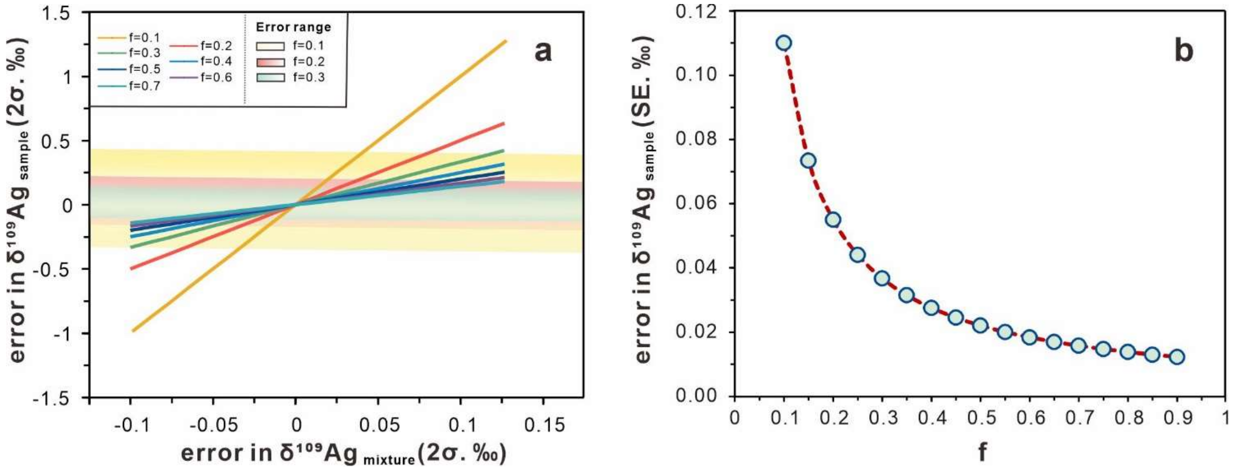

Figure 7. (a) Error propagation for δ^{109}Ag in samples as the standard deviation (2σ) from multiple measurements of δ^{109}Ag in the mixture; (b) Error propagation of δ^{109}Ag in samples as the standard error (SE) from single measurements with different proportions of silver in the sample.

h accuracy of Ag isotopic measurement and the distribution of δ^{109}Ag in the Earth

A starting point for evaluating the behaviour of silver isotopes in hydrothermal ore deposits is the silver isotopic composition of the source rocks.[29] As mentioned above, however, the very low silver abundance in silicate rocks and the high isobaric interferences for silver isotopic analysis make it difficult to reliably determine δ^{109}Ag values in silicate rocks. Using the procedure established in this study, we have been able to determine the silver isotopic composition of the ultramafic Balmuccia samples with high-precision (Table 2). Moreover, the δ^{109}Ag value of -0.044±0.062‰ obtained for the basalt reference material (BHVO-2) is consistent with the value of -0.16±0.07‰ reported by Schönbächler. [82]. In contrast to the wide distribution of δ^{109}Ag values in metallic ore-deposits, the Balmuccia ultramafic rocks have a very narrow range of δ^{109}Ag values. The orthopyroxenite (BM11-07B) and the websterite (BM11-21) have slightly negative δ^{109}Ag values of -0.038‰ and -0.031‰, which are close to the δ^{109}Ag value of -0.044‰ for BHVO-2. The spinel-clinopyroxenite has a slightly positive δ^{109}Ag value of +0.024‰. By compiling data from previous studies [22, 24-28, 30, 31, 33, 79-80], we were able to prepare histograms of δ^{109}Ag values for silver coins and hydrothermal ore-deposits. Both show normal Gaussian distributions (Figure 8a). In Figure 8b, we compare the δ^{109}Ag values of the Balmuccia ultramafic rocks and BHVO-2 to those of other terrestrial rocks. More extensive silver isotope studies of terrestrial/extra-terrestrial rocks are urgently needed to better assess the δ^{109}Ag values of the major silver reservoirs of the Earth, and to constrain sources of precious metals in polymetallic ore deposits, as well as study core formation and volatile-element depletion processes in the early solar system.

Table 2. The δ^{109}Ag for silicate rocks in the Geological Standards and Balmuccia pyroxenites

Sample no.	Sources	Rock types	Ag (ng/g)	δ^{109}Ag$_{measured}$ (‰)	2σ (n⩾4)	δ^{109}Ag$_{true}$ (‰)	2σ (n⩾4)
BM11-07B	Balmuccia	Orthopyroxenite	68.9[a]	-0.342	0.006	-0.031	0.030
BM11-21		Websterites	155.7[a]	-0.344	0.008	-0.038	0.042
BM11-27		Spinel	76.6[a]	-0.331	0.013	+0.024	0.065

		clinopyroxenites					
BHVO-2	USGS	Basalt rocks	44.4 [b]	-0.345	0.012	-0.044	0.062
				-	-	-0.16 [c]	0.07

Note: [a]The bulk-rock Ag contents are from Wang et al. [63]; [b]The Ag contents of the reference materials were obtained from Chen et al. [81]. [c] The Ag isotopic composition is from Schönbächler et al. [82].

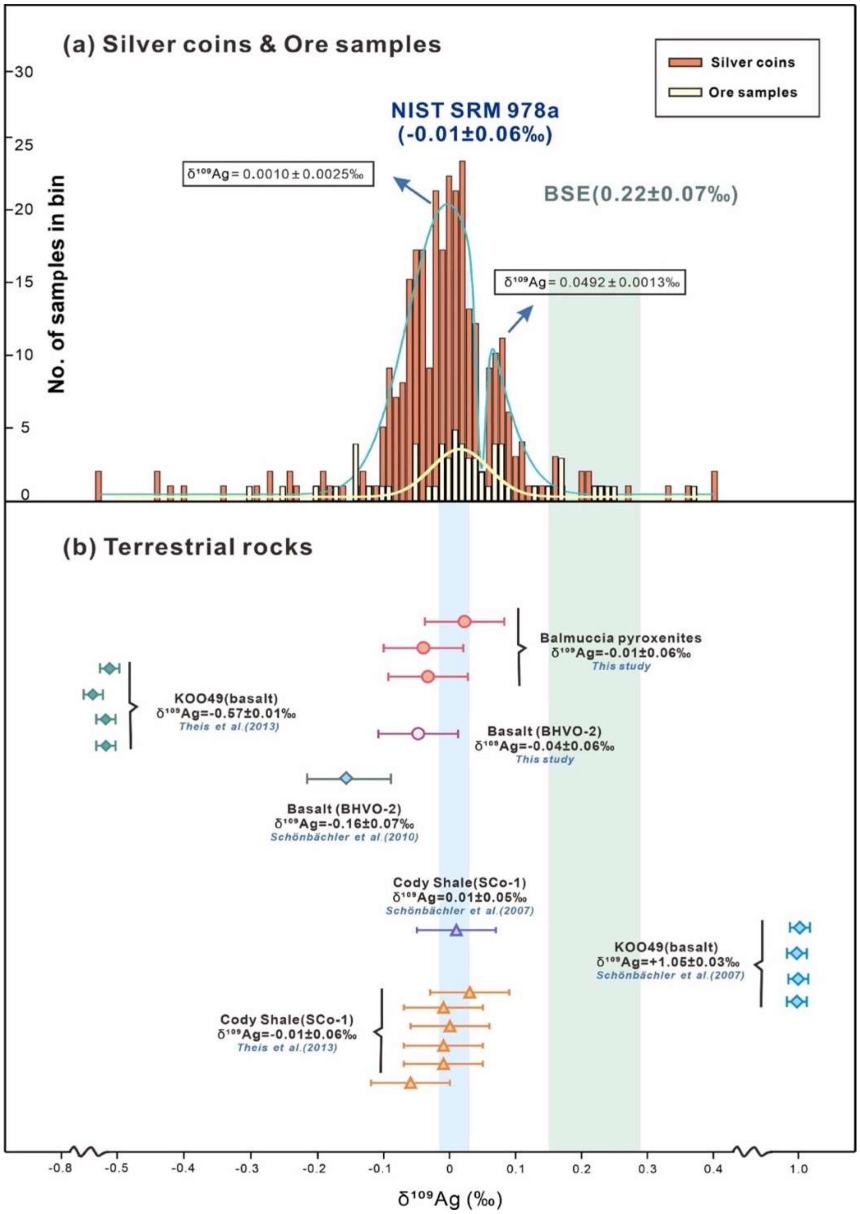

Figure 8. (a) Histograms of δ^{109}Ag values for silver coins and ore samples; (b) The distribution of δ^{109}Ag values in terrestrial rocks from values previously reported [22, 24-28, 30, 31, 33, 79-80] and in this work relative to those of the NIST SRM 978a standard and the BSE.

CONCLUSIONS

This paper presents a novel procedure for precise and accurate determinations of the silver isotopic composition of silicate rocks. The sample pre-treatment and ion exchange chromatographic protocols have been modified to ensure the efficient removal of most of the cations, especially Ti and Fe that are abundant in most silicate rocks and Ni that is abundant in mafic to ultramafic igneous rocks. Isotopic fractionation due to silver loss during ion-exchange separation and mass discrimination during instrumental analysis are adequately corrected for by the C-SSBIN approach. The matrix effects and isobaric interferences from impurities in silicate rocks were evaluated quantitatively, and evidence provided that the matrix effect induced by Ti, Cr, and Ni can be satisfactorily corrected using the proposed procedure. It was shown that there is also a noticeable shift in δ^{109}Ag, if soluble metasilicate is present in the solution. A silver standard doping method is proposed to enable accurate silver isotopic analysis of silicates with extremely low silver concentrations. The optimum doping proportion of sample to standard material is 2:8 and 40 ng·g^{-1} is the recommended minimum silver concentration in natural silicates that can be analyzed with an acceptable uncertainty. We report high-precision silver isotopic compositions for ultramafic rocks from Balmuccia and the basalt reference materials BHVO-2, all of which have δ^{109}Ag values in the range from -0.044 to +0.024 ‰. This study provides an optimal procedure for the accurate and precise silver isotopic analysis of silicate rocks.

ASSOCIATED CONTENT

Supporting Information

The Supporting Information is available free of charge on the ACS Publications website. The following information is provided: i) Abundances of metals in the upper continental crust and their molar ratios to silver; ii) Element contents in synthetic solutions of silicate samples; iii) Correlations of ln (^{109}Ag/^{107}Ag) with ln (^{i}Pd/^{j}Pd) in the doping experiments.

AUTHOR INFORMATION

Corresponding Authors: Hai-Zhen Wei

Other Authors: Yuan-Feng Zhu, Hai-Zhen Wei, Jun-Lin Wang, A. E. Williams-Jones, Zai-Cong Wang, Shao-Yong Jiang, Simon V. Hohl, Chun Huan, Miao-Miao Zhang

Notes

The authors declare no competing financial interest.

ACKNOWLEDGMENTS

This research was supported by the National Natural Science Foundations of China (Grant No. 41973005), and Research Funds for the Frontiers Science Center for Critical Earth Material Cycling, Nanjing University (Grant No. 2022300193). The authors thank Dr. Cheng Chao and Prof. Yue Cai for helpful discussions. We are grateful to the Associate Editor Prof. Sumit Chakraborty for editorial handling, and to Prof. Ryan Mathur and two anonymous reviewers for constructive and insightful comments that have significantly improved the manuscript.

REFERENCES

(1) Woodland, S. J.; Rehkämper, M.; Halliday, A. N.; Lee, D. C.; Hattendorf, B.; Günther, D. *Geochim. Cosmochim. Acta.* **2005**, 69, 2153–2163.
(2) John, D. A.; Ayuso, R. A.; Barton, M. D.; Blakely, R. J.; Vikre, P. G. Porphyry copper deposit model: Chapter B in Mineral deposit models for resource assessment, *US Geological Survey*, Reston, VA. **2010**, 5070B.
(3) Graybeal, F. T.; Vikre, P. G. *Soc. Econ. Geol.* **2010**, 1, 85–117.
(4) Kesler, S. E.; Simon, A. C. *Mineral Resources, Economics and the Environment (2nd ed.)*; Cambridge: Cambridge University Press, **2015**, pp 257-273.
(5) Rosman, K.; Taylor, P. *Pure Appl. Chem.* **1998**, 70, 217−235.
(6) Powell, L. J.; Murphy, T. J.; Gramlich, J. W. *J. Res. Natl. Bur. Stand. (U. S.).* **1982**, 87, 9−19.
(7) Prodi, V; Flynn, K. F.; Glendenin, L. E. *Phys. Rev.* **1969**, 230-232.
(8) Hauri, E. H.; Carlson, R. W. Silver isotope variations in the Earth as measured by multicollector ICP-MS, Proceedings of the Eleventh Annual V. M. Goldschmidt Conference, Hot Springs, VA, May 20−24, **2001**.
(9) Schönbächler, M.; Carlson, R. W.; Horan, M. F.; Mock, T. D.; Hauri, E. H. *Geochim. Cosmochim. Acta.* **2008**, 72, 5330–5341.
(10)Theis, K. J.; Schönbächler, M.; Benedix, G. K.; Rehkämper, M.; Andreasen, R. *Meteorit. Planet. Sci.* **2010**, 73,

433–6.

(11)Theis, K. J.; Schönbächler, M.; Benedix, G. K.; Rehkämper, M.; Andreasen, R.; Davies, C. *Earth Planet. Sci. Lett.* **2013**, 361, 402−411.

(12)Horan, M. F.; Carlson, R. W.; Blichert-Toft, J. *Earth Planet. Sci. Lett.* **2012**, 351–352, 215–222.

(13)Kruijer, T. S.; Fischer-Gödde, M.; Kleine, T.; Sprung, P.; Leya, I.; Wieler, R. *Earth Planet. Sci. Lett.* **2012**, 361, 162–172.

(14)Matthes, M.; Fischer-Gdde, M.; Kruijer, T. S.; Leya, I.; Kleine, T. *Geochim. Cosmochim. Acta.* **2015**, 169, 45–62.

(15)Righter, K.; Schnbchler, M.; Pando, K.; Rowland, R.; Lapen, T. *Earth Planet. Sci. Lett.* **2020**, 552, 116590.

(16)Tolaymat, T. M.; El Badawy, A. M.; Genaidy, A.; Scheckel, K. G.; Luxton, T. P.; Suidan, M. *Sci. Total Environ.* **2010**, 408, 999−1006.

(17)Luo, Y.; Dabek-Zlotorzynska, E.; Celo, V.; Muir, D. C. G.; Yang, L. *Anal. Chem.* **2010**, 82, 3922−3928.

(18)Yang, L.; Sturgeon, R. E.; Mester, Z.; Meija, J. *Anal. Chem.* **2010**, 82, 8978-8982.

(19)Lu, D. W.; Liu, Q.; Zhang, T. Y.; Cai, Y.; Yin, Y. G.; Jiang, G. B. *Nat. Nanotechnol.* **2016**, 11, 682.

(20)Araújo, D. F.; Boaventura, G. R.; Machado, W.; Viers, J.; Weiss, D.; Patchineelam, S. R.; Ruiz, I.; Rodrigues, A. P. C.; Babinski, M.; Dantas, E. *Chem. Geol.* **2017**, 449, 226–235.

(21)Zhang, T. Y.; Lu, D. W.; Zen, L. X.; Yin, Y. G.; He, Y. J.; Li, Q.; Jiang, G. B. *Environ. Sci. Technol.* **2017**, 51, 14164–14172.

(22)Fujii, T.; Albarède, F. *Geochim. Cosmochim. Acta.* **2018**, 234, 37–49.

(23)Milot, J.; Blichert-Toft, J.; Sanz, M. A.; Malod-Dognin, C., Télouk, P., Albarède, F. *Geology.* **2022**, 50, 422–426.

(24)Desaulty, A. M.; Telouk, P.; Albalat, E.; Albarède, F. *Proc. Natl. Acad. Sci. USA*. **2011**, 108, 9002–9007.

(25)Desaulty, A. M.; Albarède, F. *Geology.* **2013**, 41, 135-138.

(26)Albarède, F.; Blichert-Toft, J.; Rivoal, M.; Telouk, P. *Geochem. Perspect. Lett.* **2016**, 2, 127–137.

(27)Albarède, F.; Blichert-Toft, J.; de Callataÿ, F.; Davis, G.; Debernardi, P.; Gentelli, L.; Gitler, H.; Kemmers, F.; Klein, S.; Malod-Dognin, C.; Milot, J.; Télouk, P.; Vaxevanopoulos, M.; Westner, K. *Archaeometry.* **2021**, 63, 142–155.

(28)Vaxevanopoulos, M.; Davis, G.; Milot, J.; Blichert-Toft, J.; Malod-Dognin, C.; Albarède, F. *J. Archaeol. Sci.* **2022**, 145, 105645.

(29)Wang, J. L.; Wei, H. Z.; Williams-Jones, A. E.; Dong, G.; Zhu, Y. F.; Jiang, S. Y.; Ma, J.; Hohl, S. V.; Liu, X.; Li, Y. C.; Lu, J. J. *Geochim. Cosmochim. Acta.* **2022**, 332, 24–42.

(30)Mathur, R.; Arribas, A.; Megaw, P.; Wilson, M.; Stroup, S. *Geochim. Cosmochim. Acta.* **2018**, 224, 313–326.

(31)Arribas, A.; Mathur, R.; Megaw, P.; Arribas, I. *Geochem., Geophys., Geosyst.* **2020**, 21, 8.

(32)Zhu, Y. F.; Dong, G.; Liu, X.; Sheng, X. F.; Wei, H. Z. *Earth. Sci.* **2021**, 46, 4390-4404.

(33)Dong, G.; Wei, H. Z.; Zhu, Y. F.; Liu, X.; Guo, Q.; Pu, W.; Lin, Y. B.; Wang, J. L. *J. Earth. Sci.* **2022**, 33, 100–108.

(34)Gammons, C. H.; Williams-Jones, A. E. *Econ. Geol.* **1995**, 90, 420-432.

(35)Voisey, C. R.; Maas, R.; Tomkins, A. G.; Brauns, M.; Brügmann, G. *Econ. Geol.* **2019**, 114, 233–242.

(36)Boyle, R. W. *Bull. Geol. Surv. Canada*, **1979**, 280, 197.

(37)Guo, Q.; Wei, H. Z.; Jiang, S. Y.; Hohl, S.; Lin, Y. B.; Wang, Y. J.; Li, Y. C. *Anal. Chem.* **2017**, 89, 13634-13641.

(38)Savva, N. E.; Pal'Yanova, G. A.; Byankin, M. A. *Russ. Geol. Geophys.* **2012**, 53, 457-466.

(39)Seward, T. M. *Geochim. Cosmochim. Acta.* **1973**, 37, 379-399.

(40)Seward, T. M. *Geochim. Cosmochim. Acta.* **1976**, 40, 1329–1341.

(41)Shenberger, D. M.; Barnes, H. L. *Geochim. Cosmochim. Acta.* **1989**, 53, 269-278.

(42)Hayashi, K.; Ohmoto, H. *Geochim. Cosmochim. Acta.* **1991**, 55, 2111-2126.

(43)Pan, P.; Wood, S. A. *Miner. Deposita.* **1994**, 29, 373-390.

(44)Sugaki, A.; Scott, S. D.; Hayashi, K.; Kitakaze, A. *Geochem. J.* **1987**, 21, 291-305.

(45)Gammons, C. H.; Barnes, H. L. *Geochim. Cosmochim. Acta.* **1989**, 53, 279–290.

(46)Stefánsson, A.; Seward, T. M. *Geochim. Cosmochim. Acta.* **2003**, 67, 1395–1413.

(47)Argapadmi, W.; Toth, E. R.; Fehr, M. A.; Schnbchler, M. *Econ. Geol.* **2018**, 113, 1553-1570.

(48)Chen, J. H.; Wasserburg, G. J. *Geochim. Cosmochim. Acta.* **1983**, 47, 1725–1737.

(49)Kaiser, T.; Kellyw, R.; Wasserburg, G. J. *Geophys. Res. Lett.* **1980**, 7, 271–274.

(50)Kaiser, T.; Wasserburg, G. J. *Geochim. Cosmochim. Acta.* **1983**, 47, 43–58.

(51)Chen, J. H.; Wasserburg, G. J. *Geochim. Cosmochim. Acta.* **1990**, 54, 1729–1743.

(52)Chen, J. H.; Wasserburg, G. J. *Earth Processes: Reading The Isotope Code*; American Geophysical Union (AGU), **1996**; pp 1–20.

(53)Carlson, R. W.; Hauri, E. H. *Geochim. Cosmochim. Acta.* **2001**, 65, 1839–1848.

(54)Schönbachler, M.; Carlson, R. W.; Horan, M. F.; Mock, T. D.; Hauri, E. H. *Int. J. Mass Spectrom.* **2007**, 261, 183−191.

(55)Yang, L.; Dabek-Zlotorzynska, E.; Celo, V. J. *Anal. At. Spectrom.* **2009**, 24, 1564−1569.

(56)Tessalina, S. G.; Malitch, K. N.; Augé, T.; Puchkov, V. N.; Belousova, E.; McInnes, B. I. *J. Petrol.* **2015**, 56, 2297–2318.

(57)Brügmann, G.; Brauns, M.; Maas, R. *Chem. Geol.* **2019**, 516, 59–67.

(58)Wang, Z. C.; Becker, H. *Geochim. Cosmochim. Acta.* **2015**, 160, 209–226.

(59)Rudnick, R. L.; Gao, S. *Treatise. Geochem.* **2014**; 4, 1–51.

(60)Rudnick, R. L.; Gao, S. *Treatise. Geochem.* **2004**, 3, 1–65.

(61)Wang, Z. C.; Lazarov, M., Steinmann, L. K.; Becker, H.; Zou, Z.; Geng, X. L. *Am. Mineral.* **2018**, 103, 1185–1199.

(62)Wang, Z. C.; Becker, H.; Gawronski, T. *Geochim. Cosmochim. Acta.* **2013**, 108, 21–44.

(63)Wang, Z. C.; Becker, H.; Liu, Y.; Hoffmann, E.; Chen, C.; Zou, Z.; Li, Y. *Earth Planet. Sci. Lett.* **2018**, 493, 25–35.

(64)Wang, Z. C.; Becker, H. *Earth Planet. Sci. Lett.* **2015**, 417, 164–166.

(65)Wang, Z. C.; Becker, H. *Geochim. Cosmochim. Acta.* **2015**, 159, 244–263.

(66)Bos, K.; Wapstra, A. H. *Atomic Data and Nuclear Data Tables.* **1977**, 19, 277–297.

(67)Coplen, T. B.; Kendall, C. Stable hydrogen and oxygen isotope ratios for selected sites of the US Geological Survey's NASQAN and benchmark surface-water networks. *US Geological Survey*. **2000**, Open-File Report: 00–160.

(68)Pietruszka, A. J.; Reznik, A. D. *Int. J. Mass Spectrom.* **2008**, 270, 23−30.

(69)McDonough, W. F. *Treatise. Geochem.* **2003**, 2, 547–568.

(70)Wedepohl, K. H. *Geochim. Cosmochim. Acta.* **1995**, 59, 1217–1232.

(71)Wei, H. Z.; Jiang, S. Y.; Yang, T. L.; Yang, J. H.; Yang, T.; Yan, X.; Ling, B. P.; Liu, Q.; Wu, H. P. *J. Anal. At. Spectrom*. **2014**, 29, 2104–2107.

(72)Roux, P.; Lemarchand, D.; Hughes, H. J.; Turpault. M. P. *Geostand. Geoanal. Res.* **2015**, 39, 453–466.

(73)Wang, W.; Wei, H. Z.; Jiang, S. Y.; Eastoe, C. J.; Guo, Q.; Lin, Y. B. *Langmuir*. **2016**, 32, 8872–8881.

(74)Cai, Y.; Rasbury, E. T.; Wooton, K. M., Jiang, X.; Wang, D. *J. Anal. At. Spectrom.* **2021**, 36, 2153–2163.

(75)Fang, Y.; Chen, K. Y.; Bao, Z. A.; Zong, C. L.; Yuan, H. L.; Lv, N. *Anal. Chem*. **2022**, 94, 16746−16751.

(76)Rudge, J. F.; Reynolds, B. C.; Bourdon, B. *Chem. Geol.* **2009**, 265, 420−431.

(77)Patterson, K. Y.; Vellon, C.; O'Haver, T. C. *Anal. Chem.* **1994**, 66, 2829.

(78)Skrzypek, G.; Sadler, R.; Paul, D. *Rapid. Commun. Mass Spectrom.* **2010**, 24, 2697−2705.

(79) Eshel, T.; Gilboa, A.; Tirosh, O.; Erel, Y.; Yahalom-Mack, N. *J. Archaeol. Sci.* **2023**, 149, 105705.

(80) Milot, J.; Malod-Dognin, C.; Blichert-Toft, J.; Télouk, P.; Albarède, F. *Chem. Geol.* **2021**, 564, 120028.

(81) Chen, K.; Tang, M.; Lee, C.; Wang, Z. C.; Zou, Z. Q.; Hu, Z. C.; Liu, Y. S. *Earth Planet. Sci. Lett.* **2020**, 531, 115971.

(82) Schönbachler, M.; Carlson, R. W.; Horan, M. F.; Mock, T. D.; Hauri, E. H. *Science.* **2010**, 328, 884.

For Table of Contents Use Only

Manuscript title: Accurate determination of silver isotopic composition in silicate rocks with low silver abundance

Name(s) of all other authors: Yuan-Feng Zhu, Hai-Zhen Wei, Jun-Lin Wang, A. E. Williams-Jones, Zai-Cong Wang, Shao-Yong Jiang, Simon V. Hohl, Chun Huan, Miao-Miao Zhang